Supplementary Methods

Mammalian phagocytosis assay

J774 macrophages were transiently transfected in triplicate with the indicated plasmids (with GFP) in a 24-well plate or were electroporated with siRNA (see Methods) [1]. Approximately 24 hours after transfection, the cells were incubated with 1 x 10^6 TAMRA-labeled apoptotic cells (approximately 10 cells per phagocyte plated) in DMEM + 10% FBS (Cellgro). After three hours, the wells were then washed with PBS + 0.5% BSA + 1 % NaN_3 and removed from the plate with 1x Trypsin-EDTA. Cells were then stained with anti-CD3ε (UCH-T1) PE-Cy5 (Santa Cruz) and read immediately on a FACS-Caliber flow cytometer (BD Biosystems). Data was analyzed using FlowJo (TreeStar, Inc). As shown previously[1], the majority of double positive cells scored in the FACS assay represents particles engulfed by transfected cells or particles in the process of internalization, and do not represent cells simply bound to the cell surface. For siRNA experiments, J774 macrophages were stained with CFSE to differentiate phagocyte and apoptotic cell populations; for transfected cells, phagocytes were recognized by GFP fluorescence. For transfected cells, ~150,000 events were acquired; for siRNA-treated cells, ~50,000 events were acquired.

Plasmid construction

Genomic fragments corresponding to *dyn-1*, *rab-5*, *rab-7* and *nsf-1* loci were amplified by PCR from N2 genomic DNA using primers (**Supplementary Table S5**) that added an AscI site upstream and an FseI site downstream of the coding sequence (AscI - FseI cassette). All four AscI - FseI cassettes were cloned in the pCR2.1-TOPO (Invitrogen) or in pJET1 (Fermentas) vectors and sequenced to ensure fidelity. Each cassette was then excised using AscI - FseI and placed under the control of the ubiquitously expressed *eft-3* promoter and/or a *ced-1* promoter, which is expressed in all engulfing cells.

For *dyn-1*, a genomic fragment predicted to encode both protein isoforms was cloned into pLN022yfp upstream of *yfp* to generate pLS37 or into pLN022cfp upstream of *cfp* to generate pLS50. Additionally, the *eft-3* promoter originally contained in pLS37 was exchanged with a *ced-1* promoter using SbfI-AscI restriction sites to generate pKD53. For *rab-5* and *rab-7,* the amplified genomic regions were cloned into pLN019 (P_{eft-3}) or under the control of P_{ced-1} (amplified from pJMK263) and then tagged at the N-terminus of the protein with *cfp* or *yfp* to generate pKD47*(P_{eft-3}::cfp::rab-5)*, pKD38*(P_{eft-3}::yfp::rab-7)*, pKD54*(P_{ced-1}::yfp::rab-5)*, pKD55*(P_{ced-1}::yfp::rab-7)* and pKD61 *(P_{ced-1}::cfp::rab-5)* respectively.

A genomic fragment corresponding to the coding region of *nsf-1* was cloned under the control of P_{ced-1} using AscI-FseI and was then N-terminally tagged using *yfp* to generate pKD86.

The 2xFYVE domain fragment used in this study was amplified by PCR from pLN092, which contains the 2xT10G3.5(FYVE)[2] amplified as an AscI-FseI cassette and cloned under the control of the *ced-1* promoter to generate pKD58. It was then tagged at the N-terminus of the protein with *yfp* to generate pKD59.

Supplementary References

1. Tosello-Trampont, A. C., Brugnera, E. & Ravichandran, K. S. Evidence for a conserved role for CRKII and Rac in engulfment of apoptotic cells. J Biol Chem 276, 13797-802 (2001).
2. Roggo, L. et al. Membrane transport in Caenorhabditis elegans: an essential role for VPS34 at the nuclear membrane. Embo J 21, 1673-83 (2002).
3. Kamath, R. S. et al. Systematic functional analysis of the Caenorhabditis elegans genome using RNAi. Nature 421, 231-7 (2003).

Kinchen and Doukoumetzidis et al, Supplementary Figure S1

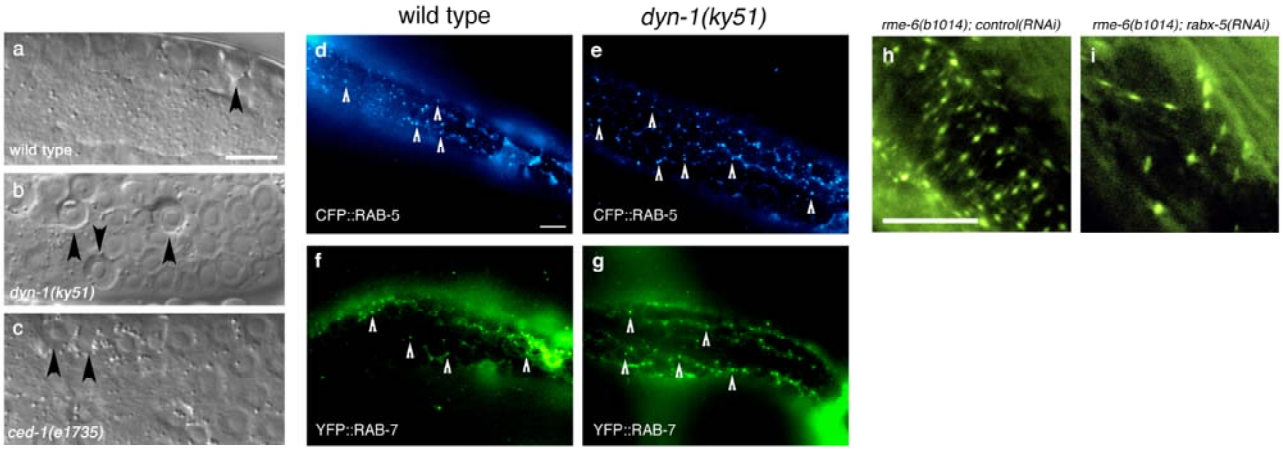

Supplementary Figure S1. RAB-5 and RAB-7 mark endocytic structures.

Arrows indicate refractile cell corpses or reporter proteins as indicated. Scale bar, 10 μm.

Phagosomes containing internalized apoptotic cells in *dyn-1(ky51)* mutant worms are larger than those found in wild type worms (**a, b**, arrowheads). Persistent uninternalized apoptotic cells in *ced-1* worms are similar to wild type (**c**). Images were quantitated using Openlab software. Quantitation is shown in **Figure 7s**. Arrowheads point to early apoptotic cells.

No decrease was detected in RAB-5 and RAB-7 staining vesicular structures in the 12-hour adult hermaphrodite gonad (arrowheads) in wild type (**d**, **f**) versus *dyn-1(ky51)* mutant worms (**e**, **g**) at the nonpermissive temperature (25 ˚C).

*(**h, i**) rme-6* and *rabx-5* are redundantly required for generation of YFP::RAB-5(+) endosomes in the somatic sheath cell (**h** vs. **i**).

Kinchen and Doukoumetzidis et al, Supplementary Figure S2

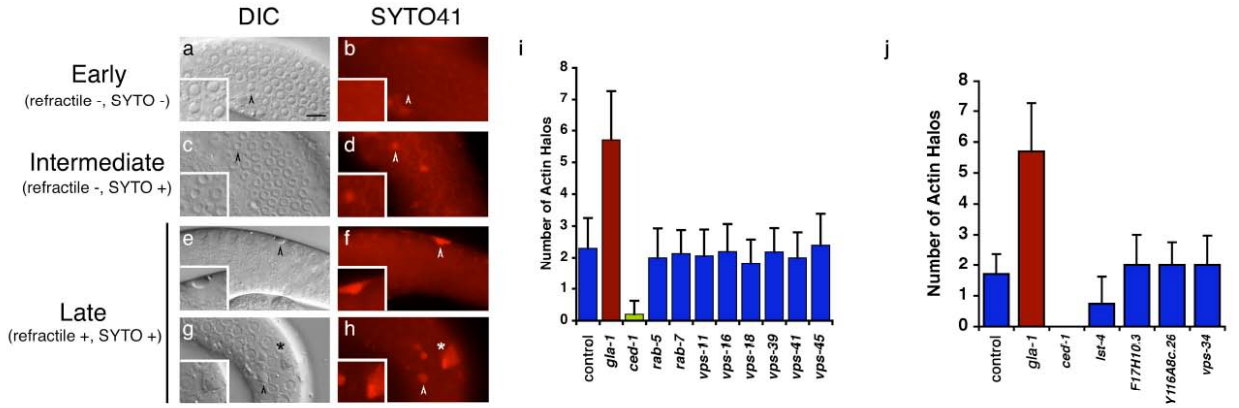

Supplementary Figure S2. Stages of engulfment and actin dynamics.

Arrowheads point to apoptotic cells. Asterisk indicates apoptotic cells potentially sharing lysosomal structures. Scale bar, 10 μm.

(**a-h**) Method used to determine corpse stage (early, intermediate or late) in Figure 1. CFP::RAB-5, YFP::RAB-7, and YFP::Actin halos are normalized to the number of early, intermediate, and late cell corpses, 'Early' apoptotic cells in the gonad begin as non-refractile SYTO41 negative bodies. After some time, these corpses progress to the 'intermediate stage' staining weakly with SYTO41 (but are still non-refractile). Finally, 'late' apoptotic cells are refractile and stain strongly with SYTO41 (**e**, **f**, **g, h**). Occasionally, multiple apoptotic cells can be seen in a single SYTO41-staining lysosome (**g**, **h**, asterisk).

(**i, j**) Actin is enriched at the membrane as the phagocyte extends its membrane around the apoptotic cell corpse; this makes actin an excellent readout to identify different defects in cell corpse removal. Increased apoptosis, such as that found in *gla-1(RNAi)* (**i**) or *gla-1(op234)* gonads (**j**), results in increased numbers of actin halos in the gonad (**i**, **j**, **red bar**). Defects in corpse internalization, such as that in *ced-1(RNAi)* worms (**i**, **j**, **green bar**) results in decreased numbers of actin halos as cell corpse engulfment (and actin recruitment) are impaired. In worms treated with RNAi against *rab-5*, *rab-7*, HOPS complex members, *vps-34* or sorting nexins, numbers of actin halos were similar to control, suggesting that corpses are efficiently engulfed in these backgrounds (**i**, **j**, **blue bars**).

Kinchen and Doukoumetzidis et al, Supplementary Figure S3

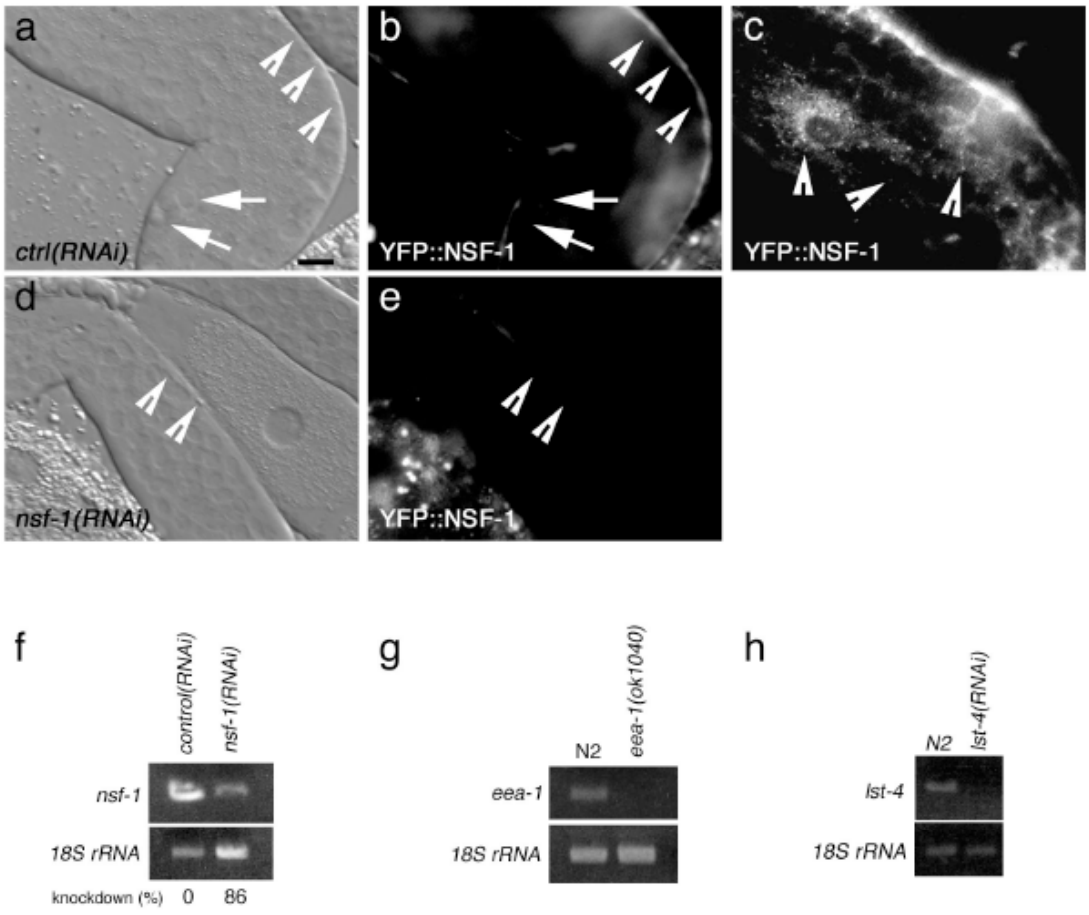

Supplementary Figure S3. Quantitation of knockdown efficiency in the somatic sheath cells.

Arrows point to apoptotic cells. Arrowheads show the somatic sheath cell (**a**, **b** and **d**, **e**) or vesicular structures in the gonad (**c**). Size bar, 10 μm.

YFP::NSF-1 is not enriched around apoptotic cells (**a**, **b**, arrows), but is localized to vesicular structures which are enriched at the perinuclear region (**c**, arrowheads). Knockdown of *nsf-1* results in a decrease in YFP::NSF-1 intensity in the gonad (**b** vs **e**). Images shown in panels (**a**,**b**) and (**d**,**e**) represent the same exposure.

Approximately 30 gonads were dissected from N2, *control(RNAi)* or *nsf-1(RNAi), lst-4(RNAi)* or *eea-1(ok1040)* worms, RNA was prepared, and cDNA generated to assess knockdown (f, h) or RNA levels of *nsf-1* (**f**), *eea-1* (**g**) or *lst-4 (***h***).*

Kinchen and Doukoumetzidis et al, Supplementary Figure S4

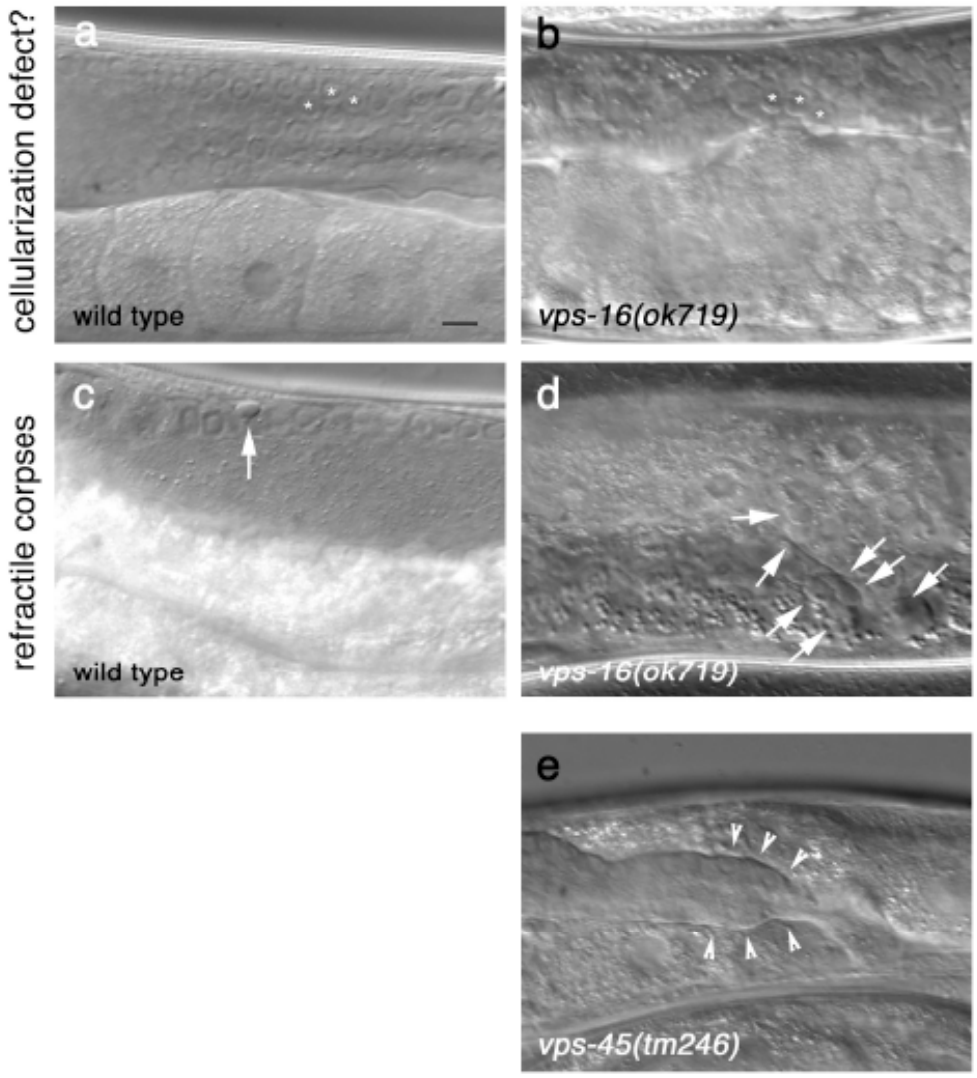

Supplementary Figure S4. *vps-16* mutant worms show multiple pleiotropic defects in the gonad.

Size bar, 10 μm. *vps-16* mutant worms show multiple defects in the gonad. In most worms, germ cells appear to cellularize early compared to wild type (**b** vs **a**). Asterisks indicate germ cell nuclei. Some worms showed 'normal' gonads, which showed increased numbers of germ cell corpses (**d**, arrows, compared to **c**). *vps-45* mutant worms showed potential mitotic defects (**e**), and germ cell corpses could not be scored.

Kinchen and Doukoumetzidis et al, Supplementary Figure S5

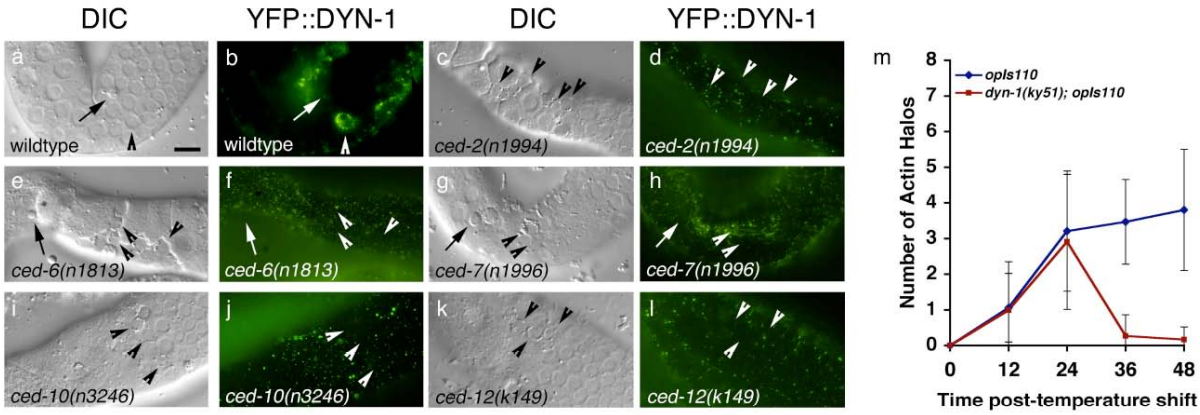

Supplementary Figure S5. DYN-1::YFP requires CED-2, CED-6, CED-7, CED-10, and CED-12 for appropriate localization in the germ line.

Arrowheads indicate early apoptotic cells; arrows indicate late, highly refractile apoptotic cells. Scale bar, 10 μm.

DYN-1::YFP is recruited around early apoptotic cells in wild-type worms (**a**, **b**, arrowheads) but not around late, highly refractile apoptotic cells (**a**, **b** arrow). In worms mutant for *ced-2* (**c**, **d**), *ced-6* (**e**, **f**), *ced-7* (**g**, **h**), *ced-10* (**i**, **j**) and *ced-12* (**k**, **l**) DYN-1 is not recruited around the apoptotic cell (arrows, arrowheads).

(**m**) Defects in corpse internalization accumulate after long-term inactivation of *dyn-1(ky51)*.

Kinchen and Doukoumetzidis et al, Supplementary Figure S6

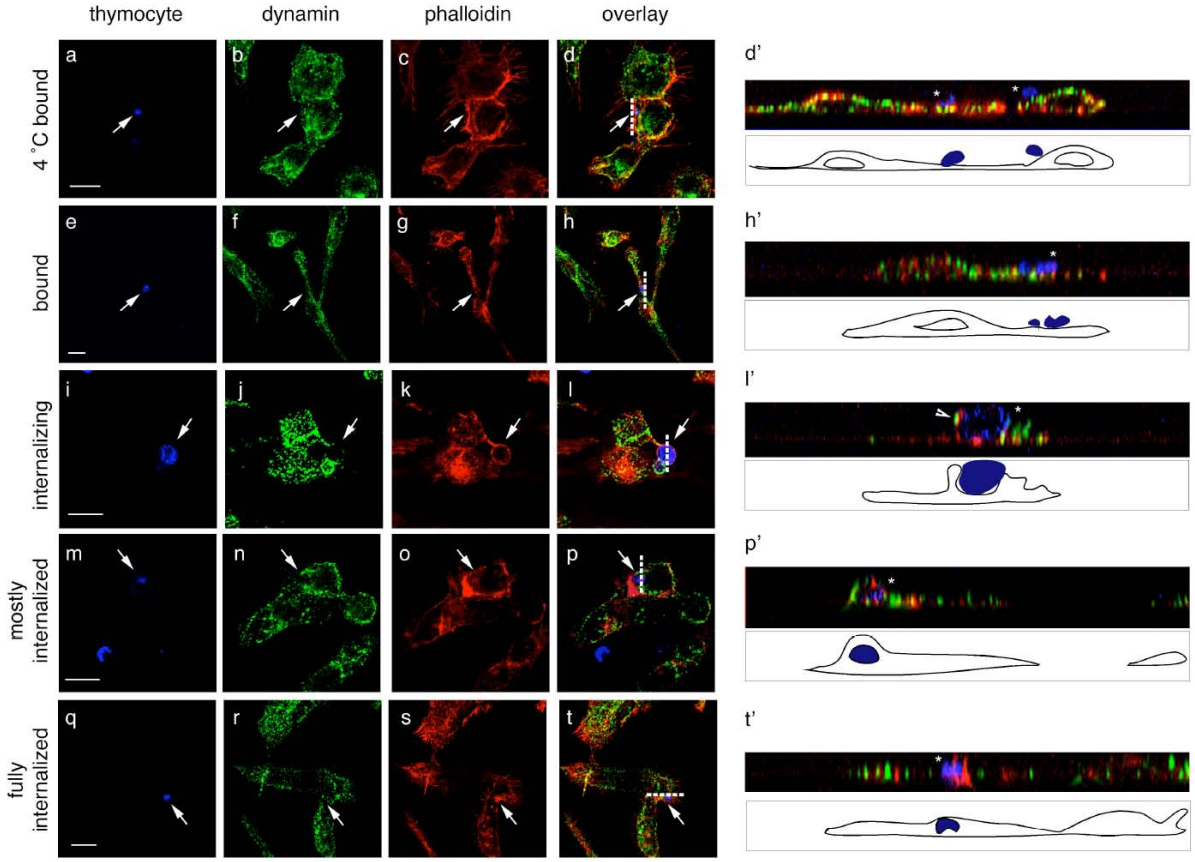

Supplementary Figure S6. Dynamin is recruited around the apoptotic cell during the internalization process.

Arrows and asterisks indicate apoptotic cells. For yz and xz reconstructions, a camera lucida tracing is included beneath the reconstruction. Scale bar, 10 μm. Dotted line indicates plane of z section.

Apoptotic cells were incubated with J774 macrophages at either 4 ˚C (**a-d, d'**) or at 37 ˚C (**e-t, h', l', p', t'**) to monitor localization of dynamin during corpse internalization. Dynamin did not localize around cells bound to the surface of macrophages (**a-h**, arrows and **d**', **h**' yz reconstruction), but was localized around apoptotic cells during pseudopod extension by the phagocytic cell (**i-p**, arrows and **l', p'**, yz reconstruction). In reconstructed sections, dynamin staining can be seen in the phagocytic cup (**l**', arrowhead) but appears excluded from the leading edge. Following internalization, dynamin staining is quickly lost (**q-t**, arrow and **t**', xz reconstruction, asterisk).

Kinchen and Doukoumetzidis et al, Supplementary Figure S7

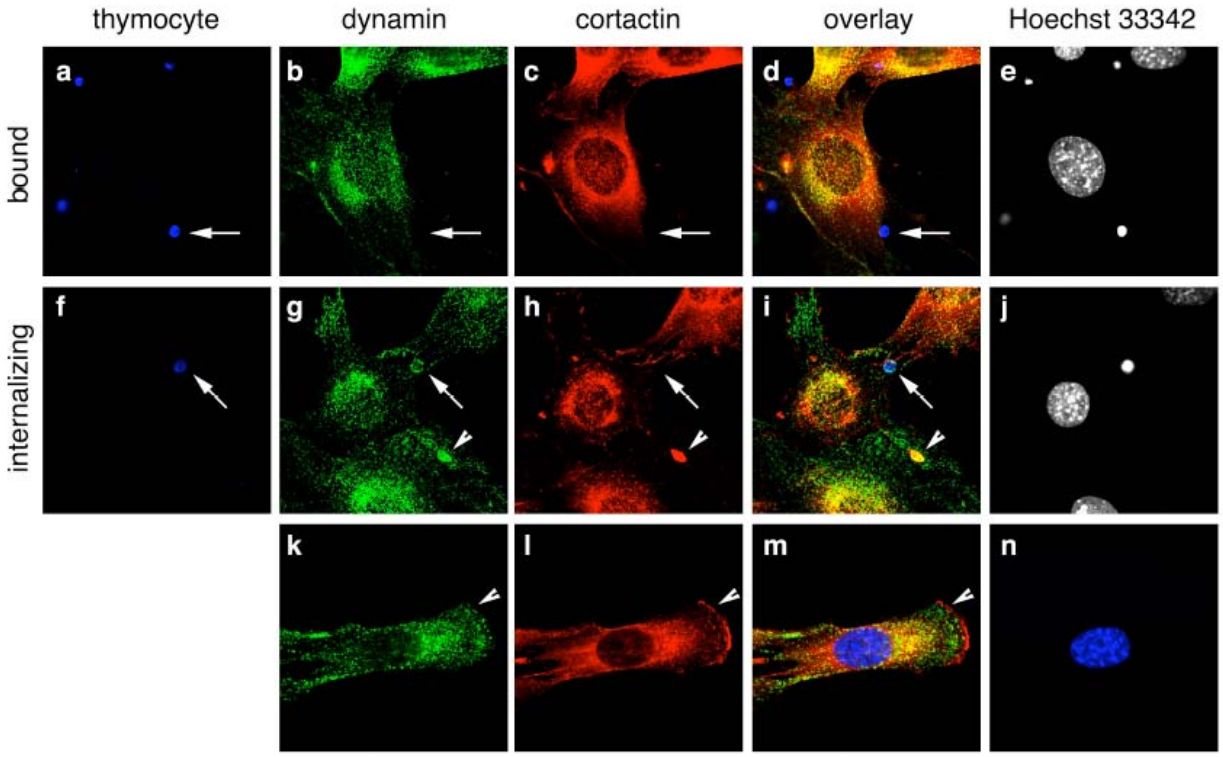

Supplementary Figure S7. Dynamin, but not the dynamin-interacting protein cortactin, is recruited to the phagocytic cup during internalization of the apoptotic cell.

Scale bar, 10 μm.

Endogenous dynamin was recruited to the phagocytic cup around cells being engulfed (**f-j,** arrow) whereas dynamin is not recruited to bound apoptotic cells (**a-e**). Endogenous cortactin could not be detected in the phagocytic cup (**f-j**) but did colocalize with endogenous dynamin in dorsal ruffle structures (**i**, arrowhead) but not in lamellipodia (**k-m**). Arrows indicate apoptotic cells. Arrowheads indicate membrane ruffles.

Kinchen and Doukoumetzidis et al, Supplementary Figure S8

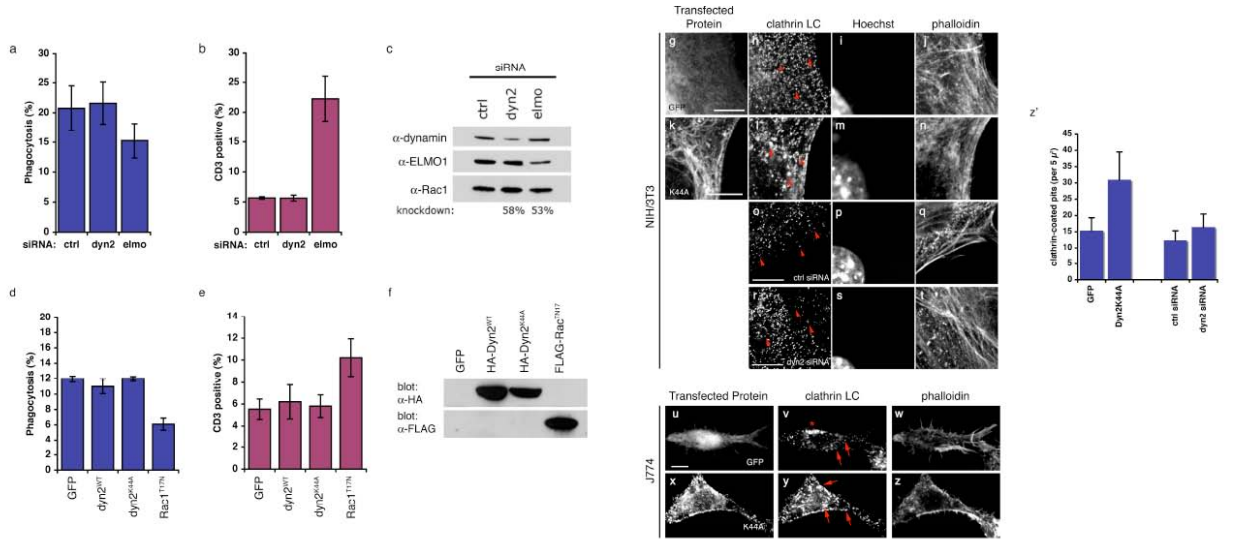

Supplementary Figure S8. Dynamin plays no detectable role in the internalization of apoptotic cells by J774 macrophages.

Scale bar, 10 μm. Arrows and arrowheads point to clathrin pits associated with endocytosed vesicles. Asterisk marks the location of Golgi body when visible in the confocal section. Data shown represent averages ± s.d.

Phagocytes were incubated with apoptotic Jurkat cells and subsequently stained cells with a fluorescently conjugated anti-CD3 antibody (see Supplementary Methods). If the phagocytic cup were still open, the anti-CD3 antibody would be free to diffuse and stain the apoptotic cell.

(**a**-**c**) J774 macrophages were transfected with control non-coding siRNA or siRNA targeting either *dynamin-2* (*dyn2*) or *elmo1* (*elmo*). Phagocytes were incubated with apoptotic Jurkat cells and subsequently stained with anti-CD3 to monitor closure of the phagocytic cup. *elmo1* knockdown decreased the efficiency of phagocytosis as well as of the membrane closure compared to control siRNA (**a, b**); there was no effect of siRNA against *dyn2*. Representative Western blot and quantitation of knockdown are shown in (**c**).

(**d**-**f**) J774 macrophages were transfected with GFP, dominant negative Dyn2^{K44A}, or dominant negative Rac^{T17N} and assayed as in (**a**-**c**). Western blot shows that all the transfected proteins were expressed (**f**).

(**g**-**z**) It was possible that we were not getting strong enough inhibition of dynamin activity. To test this, NIH/3T3 cells (**g-t**) or J774 macrophages (**u-z**) were transfected with GFP (**g-j, u-q**) or HA-Dyn2^{K44A} (**k-n, x-z**) to monitor phenotypes associated with inhibition of endocytosis. Consistent with previous observations, cells expressing Dyn2^{K44A} accumulated abnormal clathrin-coated pit structures (**l**, arrowheads and **y**, arrows) when compared to GFP-transfected cells (**h**, arrowheads and **v**, arrows). By contrast, treatment of cells with *dyn2* siRNA causes a partial loss-of-function phenotype, without accumulation of endocytic intermediates [*dyn2^{siRNA}* (**r-t**)], arrowheads compared to control siRNA (**o-q**), arrowheads].

Number of clathrin pits per 5 μ^2 shown in **z'**.

Kinchen and Doukoumetzidis et al, Supplementary Figure S9

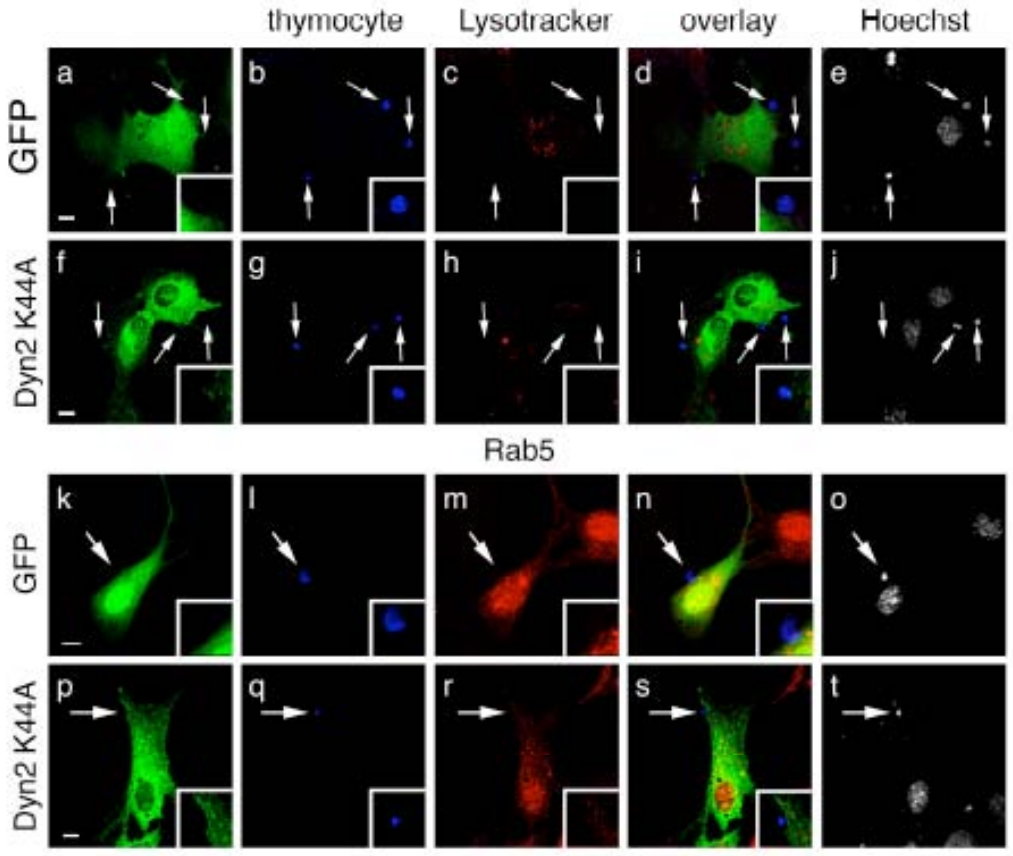

Supplementary Figure S9. Apoptotic cells incubated with phagocytes at 4 ˚C do not stain with Lysotracker Red or Rab5.

Scale bar, 10 μm.

NIH/3T3 cells incubated with apoptotic thymocytes (**b**, **g**, **l**, **q**, arrows) at 4 ˚C were stained with Lysotracker Red (**a**-**j**) or stained for endogenous Rab5 (**k**-**t**). Cells transfected with GFP (**a**, **k**) or dyn2^{K44A} (**f**, **p**) did not acquire Lysotracker Red staining (**c**, **h**, arrows and inset) or Rab5 staining (**m**, **r**, arrows and inset). Hoechst 33342 staining is additionally shown to indicate the position of the apoptotic cell nucleus (**e**, **j**, **o**, **t**, arrows). This control experiment was performed to ensure specificity of Lysotracker and Rab5 staining observed at 37˚C incubation as shown in **Figure 6** of the manuscript.

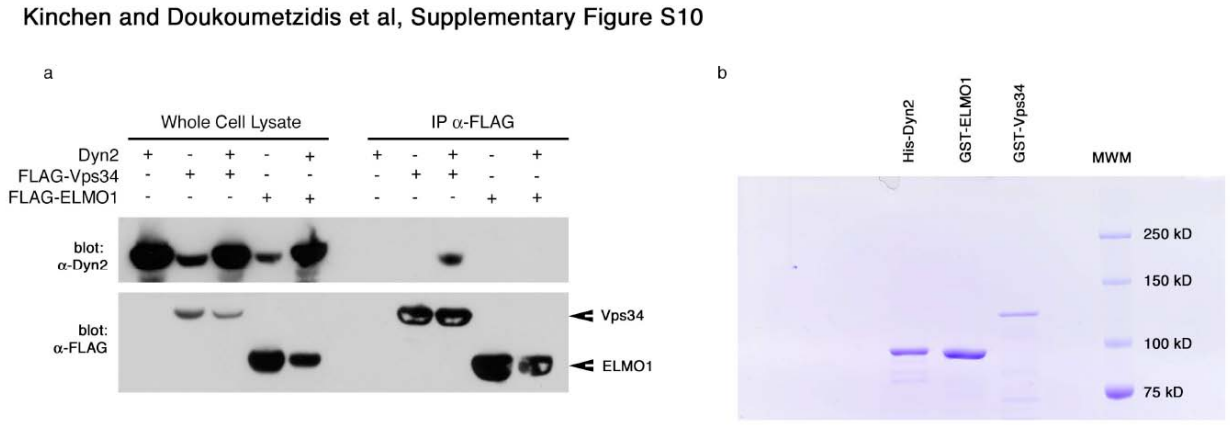

Supplementary Figure S10. Dyn2 and Vps34 can be immunoprecipitated from transfected cells.

(a) 293T cells were transfected with the indicated construct, then lysed and processed as described in Methods. IPs were run on the same gel as 20 μL of the total cell lysate to show relative 'efficiency' of Dyn2 precipitation by Vps34.

(b) Coomassie stained gel showing purified bacterially produced GST-ELMO1 and GST-Vps34 and baculovirus His-Dyn2 (gift of D. Schafer).

Supplementary Table S1. Candidate engulfment genes suppress Acridine Orange staining of apoptotic cells in the adult hermaphrodite gonad.

Data shown in 'AO Staining' column represents the fraction of worms that were AO positive (green) or AO negative (white), with the approximate penetrance of the phenotype listed. Genes were tested on three independent experiments conducted on different days to rigorously test for reproducibility. ND, not done (due to gonadal defects). Worms were staged and corpse scored as described in Methods. *n,* number of worms scored. Data shown represents average ± s.d.

Acridine orange (AO) selectively labels engulfed apoptotic germ cells. Candidate engulfment genes were identified in a feeding RNAi screen for genes, which when knocked down result in reduced AO staining in adult hermaphrodite gonads. *gla-3(op216)* mutant worms were used to increase the number of apoptotic cell corpses so that acridine orange (AO) staining could be viewed under a dissecting microscope. Identified candidates were compared to those isolated in previous screens. Candidate genes whose knockdown resulted in sterility and growth defects, which in turn could reduce the number of AO positive cells without influencing corpse removal, were excluded from further analyses and are not shown. Genes are grouped by proposed function (as identified in WormBase) as previously described[3]; genes required for actin dynamics are included in 'cell architecture.' Number of apoptotic germ cell corpses was quantitated in *gla-3(op216)* mutant worms grown on bacteria expressing the indicated construct.

Supplementary Table S1. List of candidates

Gene Model	Locus	Description	Chromosome	Refractile Corpses (DIC)	*n*	AO staining Exp.1	AO staining Exp.2	AO staining Exp.3
	gfp			8.6 ± 1.6	36	100%	100%	100%
	ced-3			0.1 ± 0.3	36	100%	100%	100%
Cell Architecture								
Y6B3A.1		Guanine nucleotide exchange factor	I	12.9 ± 5.4	36	100%	100%	100%
T23H2.5	*rab-10*	Rab-like GTPase	I	3.9 ± 2.3	12	100%	100%	100%
Y63D3A.5	*tfg-1*	Unnamed protein	I	n.d.		25% 75%	50% 50%	100%
Y71F9AM.5	*nxt-1*	RNA export factor NXT1	I	n.d.		100%	100%	100%
F08B6.4	*unc-87*	required to maintain the structure of myofilaments	I	7.3 ± 6.8	24	50% 50%	n.d.	25% 75%
F56A3.3	*npp-6*	Nuclear pore complex Nup160 compoent	I	n.d.		100%	100%	100%
F18C12.2	*rme-8*	Endocytosis function (maturation)?	I	n.d.		100%	100%	100%
Y34D9A.10	*phi-25*	Vacuolar protein sorting-associated protein 4B	I	9.5 ± 3.1	12	25% 75%	100%	25% 75%
F56A3.3	*npp-6*	Nuclear pore complex, Nup160 component	I	n.d.		100%	100%	100%
F18C12.2	*rme-8*	Endocytosis protein RME-8, contains DnaJ domain	I	n.d.		100%	100%	100%
Y79H2A.6	*arx-3*	Actin-related protein Arp2/3 complex, subunit ARPC1/p41-ARC	III	28.3 ± 10,0	24	25% 75%	25% 75%	100%
Y37D8A.1	*arx-5*	Actin-related protein Arp2/3 complex, subunit ARPC3	III	25.0 ± 9.0	24	100%	25% 75%	100%
T26A5.9	*dlc-1*	Member of the Dynein Light Chain gene class	III	9.5 ± 3.5	16	100%	100%	25% 75%
C02F4.1	*ced-5*	homolog of the human protein DOCK180	IV	16.6 ± 5.2	36	100%	100%	100%
C02C6.1	*dyn-1*	Vacuolar sorting protein VPS1	X	27.6 ± 5.6	36	100%	100%	100%
Chromatin								
F25D7.3	*blmp-1*	B Lymphocyte-induced Maturation Protein-1 homolog	I	5.5 ± 3.4	24	25% 75%	25% 75%	100%
C33H5.7		Histone H3 (Lys4) methyltransferase complex and RNA cleavage factor II complex	IV	9.3 ± 2.5	24	25% 75%	100%	n.d.

Gene Model	Locus	Description	Chromosome	Refractile Corpses (DIC)	*n*	AO staining Exp.1		Exp.2		Exp.3	
DNA Cell Cycle											
Y39G10AR.14	*mcm-4*	DNA replication licensing factor	I	5.6 ± 1.6	12	50%	50%	50%	50%	50%	50%
Y47G6A.12	*sep-1*	homolog of separase	I	9.3 ± 2.6	12	50%	50%	100%		25%	75%
W02D9.1	*pri-2*	Eukaryotic-type DNA primase, large subunit	I	n.d.		100%		100%		100%	
F32H2.3	*spd-2*	spindle defective	I	13.7 ± 3.7	36	50%	50%	50%	50%	50%	50%
Metabolism											
W01A8.4		ortholog of the NDUFB4/B15 subunit of the mitochondrial NADH dehydrogenase	I	5.0 ± 2.9	12	100%		100%		25%	75%
F25B5.6a		Folylpolyglutamate synthase	III	7.5 ± 2.9	24	100%		100%		100%	
K03H1.1		qrs-2, member of the glutaminyl (Q) tRNA Synthetase gene class	III	8.'0 ± 4.1	15	50%	50%	50%	50%	100%	
LLC1.3		orthologous to the human gene DLD	IV	1.1± 1.1	12	100%		100%		n.d.	
H04M03.4	*glf-1*	UDP-galactopyranose mutase	IV	5.0 ± 4.3	36	100%		50%	50%	n.d.	
F08C6.2		Phosphorylcholine transferase/cholinephosphate cytidylyltransferase	X	2.6 ± 1.9	12	25%	75%	100%		100%	
R04D3.1	*cyp-14A4*	Cytochrome P450 CYP2 subfamily	X	12.8 ± 3.2	24	100%		n.d.		n.d.	
Nuclei Acid Binding											
B0511.6		ATP-dependent RNA helicase pitchoune	I	n.d.		100%		100%		100%	
Neuro											
F21H11.2	*sax-2*	Fry-like conserved proteins	III	9.2 ± 2.1	21	50%	50%	100%		25%	75%
F58G6.6	*del-1*	degenerin-like	IV	9.8 ± 2.5	36	25%	75%	100%		50%	50%
C17H12.1	*dyci-1*	Cytoplasmic dynein intermediate chain	IV	8.0 ± 4.2	12	25%	75%	100%		100%	
Proteases											
F08C6.1	*adt-2*	Disintegrin metalloproteinases with thrombospondin repeats	X	n.d.		100%		100%		100%	

Gene Model	Locus	Description	Chromosome	Refractile Corpses (DIC)	*n*	AO staining Exp.1	Exp.2	Exp.3
RNA Synthesis								
Y54E10BR.6		DNA-directed RNA polymerase subunit E'	I	10.7 ± 2.3	12	100%	n.d.	100%
F14B4.3		RNA polymerase I, second largest subunit	I	n.d.		100%	100%	100%
Signaling								
B0025.1	*vps-34*	phosphoinositide 3-kinase	I	13.8 ± 4.3	36	50% 50%	50% 50%	25% 75%
Y47H9C.4	*ced-1*	homologous to human CD91	I	18.7 ± 6.8	36	100%	50% 50%	100%
F21F3.2		Glycogen synthase kinase-3	I	5.5 ± 2.1	24	50% 50%	25% 75%	50% 50%
F26E4.4		Cell Death Regulator AVEN	I	0.3 ± 0.6	12	100%	100%	100%
T23D8.9	*sys-1*	Wnt/MAPK pathway transcriptional coactivator	I	4.6 ± 2.2	12	50% 50%	100%	100%
C28A5.6		Casein kinase (serine/threonine/tyrosine protein kinase)	III	8.7 ± 4.0	21	50% 50%	100%	25% 75%
F56D2.7	*ced-6*	Src homology (SH) 3 and phosphotyrosine-binding (PTB) domain-containing adaptor protein	III	22.0 ± 9.5	24	100%	100%	100%
R144.4	*wip-1*	WASP-interacting protein	III	11.3 ± 5.9	22	50% 50%	50% 50%	50% 50%
C24A1.3		Tyrosine kinase for activated GTP-bound p21cdc42	III	12.5 ± 2.5	16	100%	100%	50% 50%
Y41D4A.5		Protein Tyrosine phosphatase	IV	10.3 ± 4.2	24	50% 50%	50% 50%	50% 50%
C45B2.7	*ptr-4*	PaTched Related family	X	3.0 ± 2.4	36	100%	100%	100%
F58A3.2	*egl-15*	Fibroblast/platelet-derived growth factor receptor and related receptor tyrosine kinases	X	11.9 ± 2.8	24	100%	100%	100%
R07E4.6	*kin-2*	cAMP-dependent protein kinase types I and II, regulatory subunit	X	n.d.		100%	100%	100%
Small Molecule Transport								
T14F9.1	*vha-15*	Vacuolar H+-ATPase V1 sector, subunit H	X	n.d.		100%	100%	100%
F59F5.1		Monocarboxylate transporter	X	9.6 ± 5.1	36	50% 50%	100%	100%

	Gene Model	Locus	Description	Chromosome	Refractile Corpses (DIC)	*n*	AO staining Exp.1		AO staining Exp.2		AO staining Exp.3	
Transcription Factors												
	F55F8.4	*cir-1*	CBF1-interacting corepressor CIR and related proteins	I	n.d.		100%		25%	75%	n.d.	
	C01H6.5	*nhr-23*	Steroid hormone nuclear receptor	I	n.d.		100%		100%		100%	
	T26A5.5		F-box protein JEMMA and related proteins with JmjC, PHD, F-box and LRR domains	III	5.5 ±4.0	21	25%	75%	25%	75%	50%	50%
	F58A4.7	*hlh-11*	Similar to transcription factor AP-4	III	6.6 ± 4.1	19	100%		100%		n.d.	
Unknown												
	C30F12.1		Uncharacterized conserved protein	I	0.8 ± 1.0	12	25%	75%	100%		25%	75%
	Y47G6A.29		unknown conserved protein	I	n.d.		100%		100%		100%	
	Y55B1BM.1	*stim-1*	mammalian stromal interaction molecule	III	6.8 ± 2.9	23	25%	75%	25%	75%	25%	75%
	Y55B1BR.2		unnamed protein	III	7.5 ± 3.6	20	50%	50%	50%	50%	n.d.	
	R07H5.4	*sdz-27*	SKN-1 Dependent Zygotic transcript)	IV	12.0 ± 3.5	36	25%	75%	25%	75%	n.d.	
	F49F1.5		Secreted surface protein	IV	11.4 ± 3.4	36	25%	75%	50%	50%	n.d.	
	F21E9.3		Uncharacterized protein with conserved cysteine	X	11.8 ± 4.2	36	50%	50%	50%	50%	n.d.	

Supplementary Table S2. Recruitment of DYN-1 around apoptotic germ cell corpses requires corpse internalization

Genotype	Refractile Corpses (DIC)	DYN-1::YFP Halos	*n*
wild type	2.7 ± 1.2	-	10
unc-119(ed3)	2.3 ± 1.1	-	10
dyn-1(ky51)	3.1 ± 1.6	-	15
opIs220 [P_{eft-3}::dyn-1::yfp]; dyn-1(ky51)	3.1 ± 1.2	-	15
wild type 25°C	3.4 ± 1.4	-	15
dyn-1(ky51) 25°C	15.9 ± 5.1	-	15
opIs220 [P_{eft-3}::dyn-1::yfp]; dyn-1(ky51) 25°C	3.9 ± 1.0	-	15
unc-119(ed3); opIs220 [P_{eft-3}::dyn-1::yfp]	3.1 ± 1.7	1.8 ± 1.1	22
ced-3(RNAi)	0	-	10
ced-3(RNAi); opIs220 [P_{eft-3}::dyn-1::yfp]	0	0	10
gla-3(op216)	7.2 ± 2.1	-	12
gla-3(op216); opIs220 [P_{eft-3}::dyn-1::yfp]	8.4 ± 2.3	2.8 ± 1.9	17
ced-1(e1735)	17.3 ± 2.7	-	15
ced-1(e1735); opIs220 [P_{eft-3}::dyn-1::yfp]	16.8 ± 2.1	0.1 ± 0.2	21
ced-6(n1813)	17.9 ± 3.3	-	15
ced-6(n1813); opIs220 [P_{eft-3}::dyn-1::yfp]	17.7 ± 3.1	0.3 ± 0.7	20
ced-7(n1996)	16.3 ± 2.3	-	13
ced-7(n1996); opIs220 [P_{eft-3}::dyn-1::yfp]	14.4 ± 2.7	0.2 ± 0.5	23
ced-2(n1994)	11.8 ± 3.5	-	20
ced-2(n1994); opIs220 [P_{eft-3}::dyn-1::yfp]	12.6 ± 4.0	0.2 ± 0.5	20
ced-5(n1812)	14.2 ± 3.0	-	15
ced-5(n1812); opIs220 [P_{eft-3}::dyn-1::yfp]	13.8 ± 2.0	0.1 ± 0.3	20
ced-12(k149)	13.0 ± 2.7	-	15
ced-12(k143); opIs220 [P_{eft-3}::dyn-1::yfp]	12.2 ± 2.6	0.2 ± 0.4	21
ced-10(n3246)	24.9 ± 4.3	-	15
ced-10(n3246); opIs220 [P_{eft-3}::dyn-1::yfp]	22.7 ± 3.9	0.5 ± 0.8	22

Worms were staged and corpses scored as described in Methods. *n,* number of worms scored. *unc-119(+)* is used as marker for transgenics. *ced-3* is the nematode caspase homologue, cell death does not occur in the gonad in *ced-3* deficient worms. Data shown are average ± s.d.

Supplementary Table S3a. Corpses are efficiently recognized and internalized in *dyn-1(ky51)* mutant worms

Genotype	Refractile Corpses (DIC)	CED-1::GFP Halos	*n*
bcIs39[P_{lim-7}::ced-1::gfp]	3.4 ± 1.9	4.1 ± 1.1	14
bcIs39[P_{lim-7}::ced-1::gfp]; dyn-1(ky51)	2.3 ± 0.9	2.9 ± 1.1	14
bcIs39[P_{lim-7}::ced-1::gfp] 25°C	4.6 ± 2.0	4.5 ± 2.5	23
bcIs39[P_{lim-7}::ced-1::gfp]; dyn-1(ky51) 25°C	12.1 ± 3.3	5.5 ± 2.0	14
	Refractile Corpses (DIC)	**YFP::Actin Halos**	
unc-119(ed3); opIs110 [P_{lim-7}::yfp::act-5]	3.9 ± 1.1	2.2 ± 1.1	14
opIs110[P_{lim-7}::yfp::act-5]; dyn-1(ky51)	4.5 ± 1.4	2.0 ± 1.2	14
ced-1(e1735); opIs110 [P_{lim-7}::yfp::act-5]	19.1 ± 5.0	0	15
unc-119(ed3); opIs110 [P_{lim-7}::yfp::act-5] 25°C	4.3 ± 2.2	3.2 ± 1.7	26
opIs110[P_{lim-7}::yfp::act-5]; dyn-1(ky51) 25°C	12.0 ± 4.9	2.9 ± 1.9	26
	Refractile Corpses (DIC)	**YFP::CED-6 Halos**	
unc-119(ed3); opIs160 [P_{ced-6}::yfp::ced-6]	3.0 ± 1.1	2.4 ± 0.8	13
opIs160 [P_{ced-6}::yfp::ced-6]; dyn-1(ky51)	3.1 ± 1.2	2.1 ± 1.0	23
unc-119(ed3); opIs160 [P_{ced-6}::yfp::ced-6] 25°C	3.6 ± 1.7	3.0 ± 1.8	13
opIs160 [P_{ced-6}::yfp::ced-6]; dyn-1(ky51) 25°C	12.9 ± 2.5	6.8 ± 1.9	23

Table S3b. Phagosome closure appears normal in *dyn-1(ky51)* mutant worms

Genotype	Refractile Corpses (DIC)	CED-1::GFP Halos	*n*
bcIs39[P_{lim-7}::ced-1::gfp] 25°C	2.2 ± 1.4	1.6 ± 1.4	13
bcIs39[P_{lim-7}::ced-1::gfp]; dyn-1(ky51) 25°C	2.6 ± 1.9	1.4 ± 1.2	14

Worms were staged and corpse scored as described in Methods. Scores shown in S3b represent average corpses in the medial plane of the gonad to monitor closure of the phagocytic cup. Data shown are average ± s.d.

Supplementary Table S4. All genes required for vesicular transport do not show defects in corpse engulfment

Genotype	Refractile Corpses (DIC)	YFP::actin (DIC)	*n*
wild type	2.7 ± 1.2	NA	10
ced-1(e1735)	17.3 ± 2.7	NA	15
rme-6(b1014)	2.4 ± 1.5	NA	13
vector(RNAi)	3.0 ± 1.4	NA	22
clic-1(RNAi)	5.6 ± 2.6	NA	24
*vector(RNAi)**	2.4 ± 1.1	NA	22
*chc-1(RNAi)**	5.9 ± 2.5	NA	22
vector(RNAi);opIs110	2.5 ± 0.9	2.0 ± 0.9	20
clic-1(RNAi);opIs110	4.2 ± 1.6	3.2 ± 1.3	20
ced-3(RNAi);opIs110	0	0	15
*vector(RNAi);opIs110**	2.2 ± 1.2	2.6 ± 1.6	20
*clhc-1(RNAi);opIs110**	4.6 ± 2.6	3.7 ± 1.9	20
*ced-3(RNAi);opIs110**	0	0	12
ret-1(gk242);vector(RNAi)	1.7 ± 0.8	NA	15
yop-1(RNAi;ret-1(gk242)	1.9 ± 0.9	NA	15
ced-3(RNAi);ret-1(gk242)	0	NA	15

Knockdown of clathrin heavy (*clhc-1*) or light (*clic-1)* result in a slight increase in numbers of apoptotic cells in the gonad. Increased corpses likely represent stress-induced apoptosis, as YFP::actin halos were also increased compared to control. Some strains (asterisks) were placed onto RNAi plates as L4 larvae due to early developmental arrest when seeded as L1 larvae. All worms were scored as 12-hour adults. *n*, number of worms scored. Error represents s.d.

Supplementary Table S5. Oligonucleotides used in this study.

RT-PCR analysis of RNA knockdown in the gonad

18S rRNA fwd	GGATAACTGCGGAAATACTGGAGC
18S rRNA rev	CAAGCGCTTGTATTGAGCACTCTG
eea-1 fwd	CGAAGGAGAAGAAACTGTGAAGCAG
eea-1 rev	GTTCAAGTTGCTCGATTGCCATCTTG
lst-4 fwd	GCTGAAGAGCTTCATCGCATATTCG
lst-4 rev	GATATTCTGATGCAGTGTAGGCGAG
nsf-1 fwd	TCAAGAAGTTCGAGTGACACCGTTC
nsf-1 rev	CGAACAAAAGAATACCTCTGACGTGC

Oligos used in construction of RNAi constructs

wdfy-2 RNAi fwd	GCAGGCGCGCCGAATCAAGTATGGGAGGAGCCAAACCAGGT
wdfy-2 RNAi rev	GCAACTAGTCTGAAAATGAGCTCGGAGGAGAGTGCAAAG
Y48E1B.14 RNAi fwd	GCAGGCGCGCCCCCCTCCATACCACCCATTCACATATTGCT
Y48E1B.14 RNAi rev	GCAACTAGTGCAGATGCAACAACAACACAACTCATTATG
Y59A8B.22 RNAi fwd	GCAGGCGCGCCTCGTCATTGTAGCTTCACCTTCACCG
Y59A8B.22 RNAi rev	GCAACTAGTGCACCGAACCGAGGAGATCAATATTG
nsf-1 RNAi fwd	GCAGGCGCGCCTGCATCTGGATCAGCTTGAGCTTTACCTCC
nsf-1 RNAi rev	GCAACTAGTCGGTGTGGAGCAAATTCAGGACTTCA

Oligos used to track deletions

rabx-5 fwd	ATT CCC CCA GAT TGT GTA TG
rabx-5 rev	TTG GTG AAC TGG TTC CGC CT
aka-1 fwd	TTCGTTCATTGGCATAATCTAACA
aka-1 rev	CTCACTCGACATCGGGAAAT
VT23B5.2 inner fwd	CCCTGAGCGAGCACTTATTC
VT23B5.2 rev	GAGATGATACATAATCACTTTCCAGC
tag-77 fwd	GTAGCTGGAGATACTAGAATAGTTGGAG
tag-77 inner rev	CGCTTATTCCGTTTGTCCAT
mtm-6 fwd	GACCCATACTACCGTACTATTCACG
mtm-6 inner rev	CCACGAAGAGGTTGCCATTT
exc-5 fwd	ATTTCCCCAAAGATCCACGG
exc-5 rev	GTGCCATCTTTTTTGGCTCC
rabs-5 fwd	GAGTTTTCCTGTTGCTGATGCTTG
rabs-5 rev	GAAGACTTTGGAGAATACGAACGACTC
eea-1 fwd	TGAACTGCGTCTTCAATTCG
eea-1 rev	GAAATCAGAGGGAATCCGGT
tag-333 fwd	GACAAACCAGCGGACAAGAT
tag-333 rev	GAAGGCGGAGAAGTGCATTA
vps-45 fwd	AATAGCGCAATAATTCCGCAC
vps-45 rev	CTAGTACATCACGCATACGGATAAT

Oligos used in constructing fluorescent reporters

AscI-Fw-dyn1	GTACGGCGCGCCatgTCGTGGCAAAACCAGGGAATG
FseI-Rv-dyn1-L	GTACGGCCGGCCGAAAGGTCTCTTGGGGACTTGCG
rab_5_Fw_AscI	TAGGGCGCGCCAAAATGGCCGCCCGAAACGCAGGAACC
rab-5_Rv_FseI	AATGGCCGGCCTTATTTACAGCATGAACCCTTTTGTTGCT
Fw_rab-7_AscI	GTACGGCGCGCCATGTCGGGAACCAGAAAGAAGGCGCT
Rv_rab-7_FseI	GTACGGCCGGCCACGGTTAACAATTGCATCCCGAATT
F_2xFYVE_AscI	GTACGGCGCGCCAGCCCACAAGCTTTGGAATTCAAATTA
R_2xFYVE_FseI	GTACGGCCGGCCTCATTTCTGGGAATCAGTGAAGCAC
Nsf-1_Fw_AscI	GTACGGCGCGCCATGAGTCCAGTCCCGTGTTTAAGCA
Nsf-1_Rv_FseI	GTACGGCCGGCCTTAACGGTACAAGTTTAGAGCAAGACC